

Stresses in FGM pressure tubes under non-uniform temperature distribution

Ahmet N. Eraslan[†]

Department of Engineering Sciences, Middle East Technical University, Ankara 06531, Turkey

(Received August 2, 2006, Accepted December 11, 2006)

Abstract. The effects of material nonhomogeneity and nonisothermal conditions on the stress response of pressurized tubes are assessed by virtue of a computational model. The modulus of elasticity, the Poisson's ratio, the yield strength, and the coefficient of thermal expansion, are assumed to vary nonlinearly in the tube. A logarithmic temperature distribution within the tube is proposed. Under these conditions, it is shown that the stress states and the magnitudes of response variables are affected significantly by both the material nonhomogeneity and the existence of the radial temperature gradient.

Keywords: pressure chamber; functionally graded material; stress analysis; von Mises' criterion.

1. Introduction

Deformation analysis of tubes subjected to either internal or external pressure is an important topic in engineering because of rigorous applications in industry as well as in daily life. For this reason, the classical problem of a long pressurized tube has been the topic of a variety of theoretical investigations. It is treated in the purely elastic stress state by Timoshenko (1956), Timoshenko and Goodier (1970), Ugural and Fenster (1987), and Boresi *et al.* (1993), in the fully plastic stress state by Boresi *et al.* (1993), Mendelson (1986), and Nadai (1931) and in the partially plastic stress state by Parker (2001) and by Perry and Aboudi (2003). Recent studies on the subject by Horgan and Chan (1999), Tutuncu and Ozturk (2001), Jabbari *et al.* (2002), Ma *et al.* (2003), and Eraslan and Akis (2005a, 2006) include tubes made of functionally graded materials (FGM) under pressure. The results of stress and deformation analyses in two layer concentric pressure tubes in the elastic state by Eraslan and Akis (2005b) and in the partially plastic stress state by the same authors (Eraslan and Akis 2004) have also been reported.

The objective of the present work is to study in detail the stress response of pressurized FGM tubes subjected to a radial temperature gradient. FGM tubes under internal pressure as well as external pressure are taken into consideration. Being different from earlier theoretical investigations (Horgan and Chan 1999, Tutuncu and Ozturk 2001, Jabbari *et al.* 2002, Ma *et al.* 2003, Eraslan and Akis 2005a, 2006) all material properties, i.e. the modulus of elasticity E , the Poisson's ratio ν , the yield strength σ_Y , and the coefficient of thermal expansion α , are assumed to vary in the tube according to the general nonlinear form

[†] Ph.D., E-mail: aeraslan@metu.edu.tr

$$F(r) = f_0[1 + G(r)] \quad (1)$$

in which f_0 is the reference value of the property F , and G is any prescribed nonlinear function of the radial coordinate r . Note that the choice $G=0$ leads to a homogeneous material property. In addition, the tube is subjected to a radial temperature gradient described by the temperature distribution

$$T(r) = \frac{\ln(r/b)T_a - \ln(r/a)T_b}{\ln(a/b)} \quad (2)$$

where a , b are the inner and outer radii, and $T_a = T(a)$, $T_b = T(b)$ are the temperatures of the inner and outer surfaces of the tube, respectively. Under these circumstances and in the framework of small deformation theory accompanied by generalized plane strain, an elastic equation is formulated in terms of formal nondimensional variables. A shooting algorithm using Newton iterations with numerically approximated tangents is designed and used for the computer solution of the elastic equation. Analytical stress and deformation expressions are also derived for a homogenous tube and used for the validation of the computational model. The results reveal that the magnitudes of the response variables as well as the stress states are affected significantly by both the material nonhomogeneity and the existence of the radial temperature gradient.

2. The elastic equation

Cylindrical polar coordinates (r, θ, z) are considered. The notation of Timoshenko and Goodier (1970) and the basic equations provided therein are employed. However, the derivation of the elastic equation is performed in terms of formal nondimensional and normalized variables for computational reasons. These variables are, radial coordinate: $\bar{r} = r/b$, bore radius: $\bar{a} = a/b$, normal stress: $\bar{\sigma}_j = \sigma_j/\sigma_Y(a)$, normal strain: $\bar{\varepsilon}_j = \varepsilon_j E_0/\sigma_Y(a)$, radial displacement: $\bar{u} = uE_0/[b\sigma_Y(a)]$, pressure: $\bar{P} = P/\sigma_Y(a)$, the coefficient of thermal expansion: $\bar{\alpha} = \alpha E_0/\sigma_Y(a)$, modulus of elasticity: $\bar{E} = E/E_0$, and the yield strength: $\bar{\sigma}_Y = \sigma_Y/\sigma_Y(a)$. The equations given below are written in terms of these variables, but to simplify the notation overbars are dropped.

A sufficiently long axisymmetric tube, a state of generalized plane strain, i.e., $\varepsilon_z = \text{constant}$, and small strains are presumed. The strain displacement relations: $\varepsilon_r = u'$, $\varepsilon_\theta = u/r$, the equation of equilibrium in radial direction: $\sigma_\theta = (r\sigma_r)'$ and the equations of generalized Hooke's law of the form

$$\varepsilon_i = \frac{1}{E}[\sigma_i - \nu(\sigma_j + \sigma_k)] + \alpha T \quad (3)$$

constitute the basis for the formulation (Timoshenko and Goodier 1970, Ugural and Fenster 1987, Boley and Weiner 1960). In above, a prime indicates differentiation with respect to nondimensional radial coordinate r . In a state of generalized plane strain the axial stress reads

$$\sigma_z = E\varepsilon_z + \nu(\sigma_r + \sigma_\theta) - E\alpha T \quad (4)$$

Introducing the stress function $Y(r)$ in terms of radial stress as $Y(r) = r\sigma_r$, one obtains from the equation of equilibrium $\sigma_\theta = Y'(r)$. Eliminating the axial stress σ_z from the equations of Hooke's law, and using the stress function $Y(r)$ the total strains become

$$\varepsilon_r = \frac{1}{E} \left[\frac{(1-\nu^2)}{r} Y - \nu(1+\nu) Y' \right] + (1+\nu) \alpha T - \nu \varepsilon_z \quad (5)$$

$$\varepsilon_\theta = -\frac{1}{E} \left[\frac{\nu(1+\nu)}{r} Y - (1-\nu^2) Y' \right] + (1+\nu) \alpha T - \nu \varepsilon_z \quad (6)$$

The elastic equation is obtained by the substitution of Eqs. (5) and (6) in the compatibility relation $(r\varepsilon_\theta)' = \varepsilon_r$. The result is

$$\begin{aligned} \frac{d^2 Y}{dr^2} + \left[\frac{1}{r} - \frac{1}{E} \frac{dE}{dr} - \frac{2\nu}{1-\nu^2} \frac{d\nu}{dr} \right] \frac{dY}{dr} - \left[\frac{1}{r} - \frac{\nu}{E(1-\nu)} \frac{dE}{dr} + \frac{1+2\nu}{1-\nu^2} \frac{d\nu}{dr} \right] \frac{Y}{r} \\ = \frac{E}{1-\nu^2} [\varepsilon_z - \alpha T] \frac{d\nu}{dr} - \frac{E}{1-\nu} \left[\alpha \frac{dT}{dr} + \frac{d\alpha}{dr} T \right] \end{aligned} \quad (7)$$

The solution of this equation provides elastic stresses in plane strain axisymmetric problems with nonuniform temperature field and graded material properties. Although it is a linear ODE, the coefficients of Y and Y' are so complicated that its closed form solution could not be found. However, accurate numerical solutions can be obtained by the use of shooting method as described in the next section.

Note that for a homogeneous material $E' = 0$; $E = 1$, and $\nu' = 0$; $\nu = \nu_0$, and $\alpha = \alpha_0$, Eq. (7) is ultimately simplified to

$$r^2 \frac{d^2 Y}{dr^2} + r \frac{dY}{dr} - Y = -\frac{\alpha_0}{1-\nu_0} r^2 \frac{dT}{dr} \quad (8)$$

which is nothing but the classical plane strain thermoelastic equation of Cauchy-Euler nonhomogeneous type (Ugural and Fenster 1987).

2.1 The shooting method

First, Eq. (7) is cast into the form

$$\frac{d^2 Y}{dr^2} = F\left(r, Y, \frac{dY}{dr}\right) \quad (9)$$

Then, making use of the fact that $\sigma_\theta = Y'$, Eq. (9) is transformed into an initial value problem (IVP)

$$\frac{dY}{dr} = \sigma_\theta \quad (10)$$

$$\frac{d\sigma_\theta}{dr} = F(r, Y, \sigma_\theta) \quad (11)$$

in $a \leq r \leq 1$ subjected to the initial values

$$Y(a) = Y_a; \quad \sigma_\theta(a) = \left. \frac{dY}{dr} \right|_{r=a} \quad (12)$$

The initial value Y_a is known. It is $Y_a = -a \times P$ in case of internal pressure, and it is $Y_a = 0$ in case of external pressure. However, the gradient $dY/dr|_{r=a}$ is not known. This gradient can be computed iteratively using Newton's method accompanied by the boundary condition $Y(1)$. Having X_{k-1} and Δ

denote the value of $dY/dr|_{r=a}$ at iteration number $k-1$, and a small increment of the order 10^{-3} , respectively, we perform 3 runs in every iteration to generate the gradient in Newton's equation. In case of internal pressure $Y_a = -a \times P$ throughout, and at the k -th iteration we perform runs

1. starting with X_{k-1} to obtain $f_1 = Y(1)$,
2. starting with $X_{k-1} + \Delta$ to obtain $f_2 = Y(1)$,
3. starting with $X_{k-1} - \Delta$ to obtain $f_3 = Y(1)$.

A better approximation for $dY/dr|_{r=a}$ can now be obtained from

$$\left. \frac{dY}{dr} \right|_{r=a} = X_k = X_{k-1} - \frac{2\Delta f_1}{f_2 - f_3} \quad (13)$$

Iterations are repeated until $|X_k - X_{k-1}|$ is less than a specified error tolerance. If the tube is subjected to external pressure P , then $Y_a = 0$ all the way through, and the runs

1. starting with X_{k-1} to obtain $f_1 = Y(1) + P$,
2. starting with $X_{k-1} + \Delta$ to obtain $f_2 = Y(1) + P$,
3. starting with $X_{k-1} - \Delta$ to obtain $f_3 = Y(1) + P$,

are carried out to successively improve $dY/dr|_{r=a}$ by virtue of Eq. (13).

On the other hand, an outer iteration loop is performed to estimate the value of ε_z . An iteration scheme similar to those given above is constructed. At each main iteration, the problem is solved three times using ε_z^{k-1} , $\varepsilon_z^{k-1} + \Delta_\varepsilon$ and $\varepsilon_z^{k-1} - \Delta_\varepsilon$ respectively, and the corresponding net axial forces $\int \sigma_z dA$ are calculated. Here, dA refers to an area element on the cross section. Aiming at $\int \sigma_z dA = 0$, a better approximation ε_z^k to the constant axial strain is then obtained from

$$\varepsilon_z^k = \varepsilon_z^{k-1} - \frac{2\Delta \int \sigma_z(\varepsilon_z^{k-1}) dA}{\int \sigma_z(\varepsilon_z^{k-1} + \Delta_\varepsilon) dA - \int \sigma_z(\varepsilon_z^{k-1} - \Delta_\varepsilon) dA} \quad (14)$$

Starting with a reasonable initial estimate ε_z^0 , this iteration scheme converges to the result with a sufficient accuracy only in a few iterations. The result of a homogeneous calculation, for example, provides a good initial estimate ε_z^0 . The advantages of this procedure are stability, rate of convergence and availability of state-of-the-art ODE solvers (Brown and Hindmarsh 1989) for accurate integrations.

3. Analytical stresses and limits

These stresses are based on the general solution of Eq. (8). Substituting $T(r)$ as given by Eq. (2), and integrating Eq. (8) one arrives at

$$Y(r) = \frac{C_1}{r} + C_2 r + \frac{\alpha_0(T_b - T_a)r \ln r}{2(1 - \nu_0) \ln a} \quad (15)$$

where C_1 and C_2 are arbitrary constants to be determined. The stresses and radial displacement then become

$$\sigma_r = \frac{C_1}{r^2} + C_2 + \frac{\alpha_0(T_b - T_a)\ln r}{2(1 - \nu_0)\ln a} \quad (16)$$

$$\sigma_\theta = -\frac{C_1}{r^2} + C_2 + \frac{\alpha_0(T_b - T_a)(1 + \ln r)}{2(1 - \nu_0)\ln a} \quad (17)$$

$$\sigma_z = -\frac{\alpha_0}{2(1 - \nu_0)\ln a} \{ (2\ln r + \nu_0)T_a + [2\ln(a/r) - \nu_0(1 + 2\ln a)]T_b \} + 2C_2\nu_0 + \varepsilon_z \quad (18)$$

$$u = (1 + \nu_0) \left[-\frac{C_1}{r} + (1 - 2\nu_0)rC_2 \right] + \frac{\alpha_0(1 + \nu_0)r}{2(1 - \nu_0)\ln a} (D_1 - D_2) - \varepsilon_z \nu_0 r \quad (19)$$

where the dummy variables have been defined as

$$D_1 = [(1 - \nu_0)(1 + 2\ln a) - \ln r]T_b \quad (20)$$

$$D_2 = (1 - \nu_0 - \ln r)T_a \quad (21)$$

3.1 Internal pressure

The use of the conditions

$$\sigma_r(a) = -P, \quad \sigma_r(1) = 0, \quad \text{and} \quad \int_a^1 \sigma_z dA = 2\pi \int_a^1 \sigma_z r dr = 0 \quad (22)$$

leads to

$$C_1 = \frac{a^2 P}{a^2 - 1} + \frac{a^2 \alpha_0 (T_b - T_a)}{2(a^2 - 1)(1 - \nu_0)} \quad (23)$$

$$C_2 = -\frac{a^2 P}{a^2 - 1} - \frac{a^2 \alpha_0 (T_b - T_a)}{2(a^2 - 1)(1 - \nu_0)} \quad (24)$$

$$\varepsilon_z = \frac{2a^2 \nu_0 P}{a^2 - 1} - \frac{\alpha_0}{2(a^2 - 1)\ln a} [(1 - a^2 + 2\ln a)T_b - (1 - a^2 + 2a^2 \ln a)T_a] \quad (25)$$

On the other hand, earlier studies (see, for example, Eraslan and Akis 2005a) indicate that the inner surface of the tube is critical; consequently, the homogeneous pressure tube fails with respect to plastic flow at this location as soon as the internal pressure reaches a limiting value P_E called the elastic limit pressure. This limit can be calculated by the use of the von Mises' criterion. For plane strain this criterion takes the form (Eraslan and Akis 2006)

$$\phi_Y = \sqrt{\frac{1}{2} [(\sigma_r - \sigma_\theta)^2 + (\sigma_r - \sigma_z)^2 + (\sigma_\theta - \sigma_z)^2]} \quad (26)$$

The tube undergoes plastic deformation when $\phi_Y(a) = 1$. Evaluating the stresses explicitly from Eqs. (16)-(18) at $r = a$ with the aid of Eqs. (23)-(25) and substituting in Eq. (26), we obtain after some algebraic manipulations

$$P_E = \frac{\alpha_0(T_a - T_b)D_3 + \sqrt{D_4 - 3\alpha_0^2(T_a - T_b)^2D_5}}{D_6} \quad (27)$$

where

$$D_3 = (3 - a^2)(1 - a^2 + 2\ln a)\ln a \quad (28)$$

$$D_4 = 16(1 - a^2)^2(3 + a^4)(1 - \nu_0)^2\ln^4 a \quad (29)$$

$$D_5 = [(1 - a^2 + 2\ln a)(1 + a^2)\ln a]^2 \quad (30)$$

$$D_6 = 4(3 + a^4)(1 - \nu_0)\ln^2 a \quad (31)$$

3.2 External pressure

In case the tube is subjected to external pressure, the conditions to be used read

$$\sigma_r(a) = 0, \quad \sigma_r(1) = -P, \quad \text{and} \quad \int_a^1 \sigma_z r dr = 0 \quad (32)$$

Application of these results in

$$C_1 = -\frac{a^2 P}{a^2 - 1} + \frac{a^2 \alpha_0 (T_b - T_a)}{2(a^2 - 1)(1 - \nu_0)} \quad (33)$$

$$C_2 = \frac{P}{a^2 - 1} - \frac{a^2 \alpha_0 (T_b - T_a)}{2(a^2 - 1)(1 - \nu_0)} \quad (34)$$

$$\varepsilon_z = -\frac{2\nu_0 P}{a^2 - 1} - \frac{\alpha_0}{2(a^2 - 1)\ln a} [(1 - a^2 + 2\ln a)T_b - (1 - a^2 + 2a^2\ln a)T_a] \quad (35)$$

Like in the internal pressure case, the tube plasticizes at the inner surface as soon as $\phi_1(a) = 1$. Accordingly, the elastic limit pressure is determined as

$$P_E = \frac{\alpha_0(T_a - T_b)D_7 - \sqrt{D_8 - 3\alpha_0^2(T_a - T_b)^2D_9}}{D_{10}} \quad (36)$$

where

$$D_7 = (1 - a^2 + 2\ln a)\ln a \quad (37)$$

$$D_8 = 16(1 - a^2)^2(1 - \nu_0)^2\ln^4 a \quad (38)$$

$$D_9 = [(1 - a^2 + 2\ln a)\ln a]^2 \quad (39)$$

$$D_{10} = -8(1 - \nu_0)\ln^2 a \quad (40)$$

4. Results and discussion

In all of the following calculations $\nu_0 = 0.3$, and $\alpha = \alpha_0 = 5.85 \times 10^{-3}/^\circ\text{C}$. Furthermore, double precision (16-digit) arithmetic is used in the numerical computations.

4.1 Verification of the computational model

The computational model can be verified in comparison to the analytical results. For this purpose, the material properties $E = 1$, $\sigma_Y = 1$, $\nu = \nu_0$, and $\alpha = \alpha_0$ accompany the numerical solutions. First, a long tube of inner radius $a = 0.7$ subjected to internal pressure is considered. Assigning $T_a = 5^\circ\text{C}$, and $T_b = 28^\circ\text{C}$, i.e., $\Delta T = T_b - T_a > 0$, from Eq. (27) the elastic limit pressure is calculated as $P_E = 0.261264$. Furthermore, by virtue of Eqs. (23)-(25) we evaluate the corresponding analytical constants as $C_1 = -0.343357$, $C_2 = 0.343357$, and $\varepsilon_z^0 = -4.61547 \times 10^{-2}$. For the same tube under $P_E = 0.261264$ a run is performed starting with $\varepsilon_z^0 = -4.0 \times 10^{-2}$, and $X_0 = 0.8$. Iterations are repeated until $\int \sigma_z dA < 10^{-10}$. When the iterations converge after 2 iterations, there results $\int \sigma_z dA = 2.21 \times 10^{-14}$, $\varepsilon_z = -4.61547 \times 10^{-2}$, and $X = 0.870739$. The corresponding distributions of response variables are plotted in Fig. 1(a). In this figure, solid lines belong to numerical solution, and dots to analytical solution by the use of Eqs. (16)-(19). The nondimensional stress variable Φ in Fig. 1(a) is calculated from

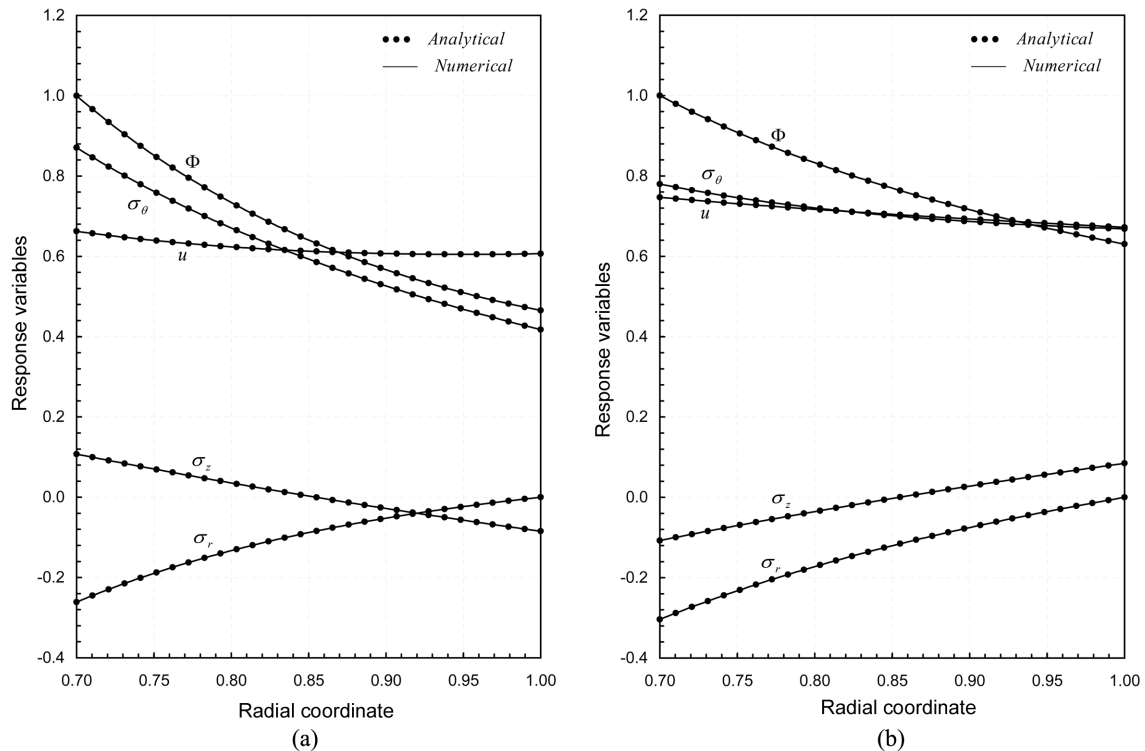


Fig. 1 The elastic response of a homogeneous tube of $a = 0.7$ subjected to internal pressure. (a) For $T_a = 5^\circ\text{C}$, $T_b = 28^\circ\text{C}$, under elastic limit pressure $P = P_E = 0.261264$, (b) for $T_a = 28^\circ\text{C}$, $T_b = 5^\circ\text{C}$, under elastic limit pressure $P = P_E = 0.303711$. Solid lines show numerical, dots analytical results

$$\Phi = \frac{1}{\sigma_Y \sqrt{2}} \sqrt{\frac{1}{2} [(\sigma_r - \sigma_\theta)^2 + (\sigma_r - \sigma_z)^2 + (\sigma_\theta - \sigma_z)^2]} \quad (41)$$

Both solutions agree perfectly. In fact, in all calculated, analytical and numerical solutions agree to at least 6 significant digits. Note also that, according to von Mises' yield criterion, Eq. (26), $\Phi = 1$ at the plastic-elastic border, and $\Phi < 1$ in the elastic region. Hence, Φ turns out a useful global variable not only in monitoring the material failure with respect to yield, but also in measuring the error in stress calculations. Following the variation of Φ in Fig. 1(a), we see that the tube fails at the inner surface since $\Phi = 1$ at this location. What is more, the stresses in the tube satisfy $\sigma_\theta > \sigma_z > \sigma_r$ in the inner portion and $\sigma_\theta > \sigma_r > \sigma_z$ in a relatively narrower outer portion. For $a = 0.7$, similar calculations are carried out by reversing the temperature gradient. This time we take $T_a = 28^\circ\text{C}$, and $T_b = 5^\circ\text{C}$ ($\Delta T < 0$) and determine $P_E = 0.303711$, $C_1 = -0.199462$, $C_2 = 0.199462$, and $\varepsilon_z = -8.64867 \times 10^{-2}$. Numerical solution for this problem converges in 3 iterations resulting in $\int \sigma_z dA = 3.29 \times 10^{-15}$, $\varepsilon_z = -8.64867 \times 10^{-2}$, and $X = 0.779874$. The consequent analytical (dots) and numerical (solid lines) stresses are compared in Fig. 1(b). Again, perfect agreement is obtained. The stress state is $\sigma_\theta > \sigma_z > \sigma_r$ throughout. Comparison of Figs. 1(a) and (b) reveals how the stress states are affected by the existence of a small temperature gradient, which is likely to occur in pressure chambers.

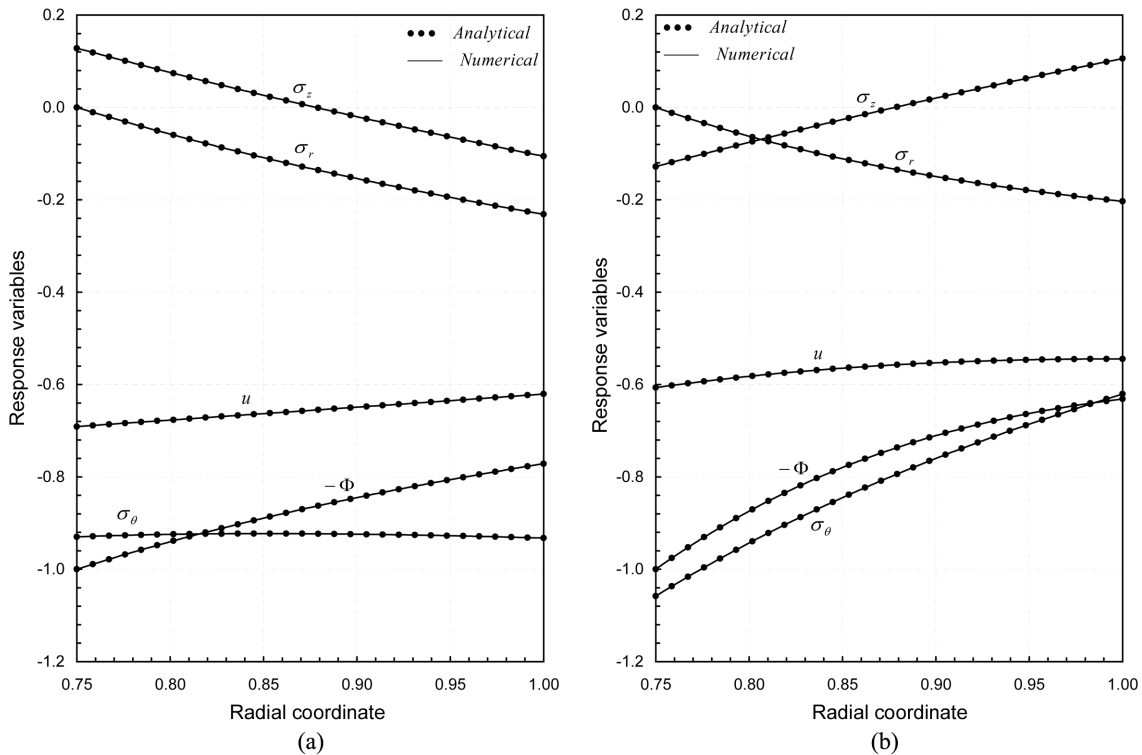


Fig. 2 The elastic response of a homogeneous tube of $a = 0.75$ subjected to external pressure. (a) For $T_a = 8^\circ\text{C}$, $T_b = 36^\circ\text{C}$, under elastic limit pressure $P = P_E = 0.231416$, (b) for $T_a = 36^\circ\text{C}$, $T_b = 8^\circ\text{C}$, under elastic limit pressure $P = P_E = 0.203381$. Solid lines show numerical, dots analytical results

Next the tubes under external pressure are studied. A tube of inner radius $a = 0.75$ subjected to surface temperatures of $T_a = 8^\circ\text{C}$, and $T_b = 36^\circ\text{C}$ ($\Delta T > 0$) is considered first. From Eqs. (36), and (33)-(35), in turn, we calculate $P_E = 0.231416$, $C_1 = 0.147106$, $C_2 = -0.378522$, and $\varepsilon_z = 0.453881$. On the other hand, the numerical solution gives $\int \sigma_z dA = -4.37 \times 10^{-15}$, $\varepsilon_z = 0.453881$, and $X = -0.929743$ after 2 main iterations. Fig. 2(a) shows the corresponding analytical (dots) and numerical (solid lines) distributions of response variables. Both solutions agree perfectly. Also, the stresses satisfy $\sigma_z > \sigma_r > \sigma_\theta$ all the way through. If the surface temperatures are assigned as $T_a = 36^\circ\text{C}$, and $T_b = 8^\circ\text{C}$ ($\Delta T < 0$) there results $P_E = 0.203381$, $C_1 = 0.411919$, $C_2 = -0.615300$, and $\varepsilon_z = 0.399812$ analytically, and $\int \sigma_z dA = -1.29 \times 10^{-14}$, $\varepsilon_z = 0.399812$, and $X = -1.05790$ numerically. The corresponding distributions of stress and displacement are plotted in Fig. 2(b). Again, dots show analytical profiles. The stress state is different from that of $\Delta T > 0$, and it is $\sigma_r > \sigma_z > \sigma_\theta$ in the inner, and $\sigma_z > \sigma_r > \sigma_\theta$ in the outer portions of the tube, respectively. These calculations indicate that the numerical solution algorithm converges very rapidly, leads to solutions possessing high order accuracy, and also that the computer program which implements this algorithm functions properly.

4.2 Analysis of FGM tubes

4.2.1 Internal pressure

First, a parametric analysis is carried out to ascertain the effect of each of the variable material properties on the elastic limit pressure P_E . For this purpose, a tube of inner radius $a = 0.7$, and small temperature gradients, on the order of 25°C , are considered. Material properties E , ν , and α are allowed to vary nonlinearly within the tube one at a time while the others are kept constant. The results of these calculations are summarized in Table 1. The yield strength σ_Y is not included in this table, because, as will be shown later in this section, its effect on the performance of the pressure tube is somewhat different, yet important, and thus cannot be evaluated by simply weighing P_E . As seen in Table 1, the elastic limit increases for both positive and negative temperature gradients if the modulus of elasticity E is an increasing function of the radial coordinate r . The increase in either ν or α from $r = a$ to $r = 1$, however, causes the elastic limit to decrease as shown. Although all affect the elastic response of the tube to some extent, the effect of E is observed to be highly pronounced as expected.

As seen in Fig. 1, a homogeneous tube subjected to internal pressure always yields at the inner surface. However, in case the tube material is nonhomogeneous, it may undergo plasticization at the outer, or simultaneously at both of the surfaces. To illustrate these different modes of incipient yielding, we consider a tube of inner radius $a = 0.7$ and assign $T_a = 5^\circ\text{C}$ and $T_b = 30^\circ\text{C}$. The material composition shown in Fig. 3(a) is taken into account. The nonlinear functions that describe the variations of the properties are noted at the bottom of Fig. 3(a). This material composition gives rise

Table 1 Effect of variable E , ν , and α , respectively, on the elastic limit pressure P_E

Property	$\Delta T > 0$	$\Delta T < 0$
$E(a) < E(1)$	$P_E \uparrow$	$P_E \uparrow$
$\nu(a) < \nu(1)$	$P_E \downarrow$	$P_E \downarrow$
$\alpha(a) < \alpha(1)$	$P_E \downarrow$	$P_E \downarrow$

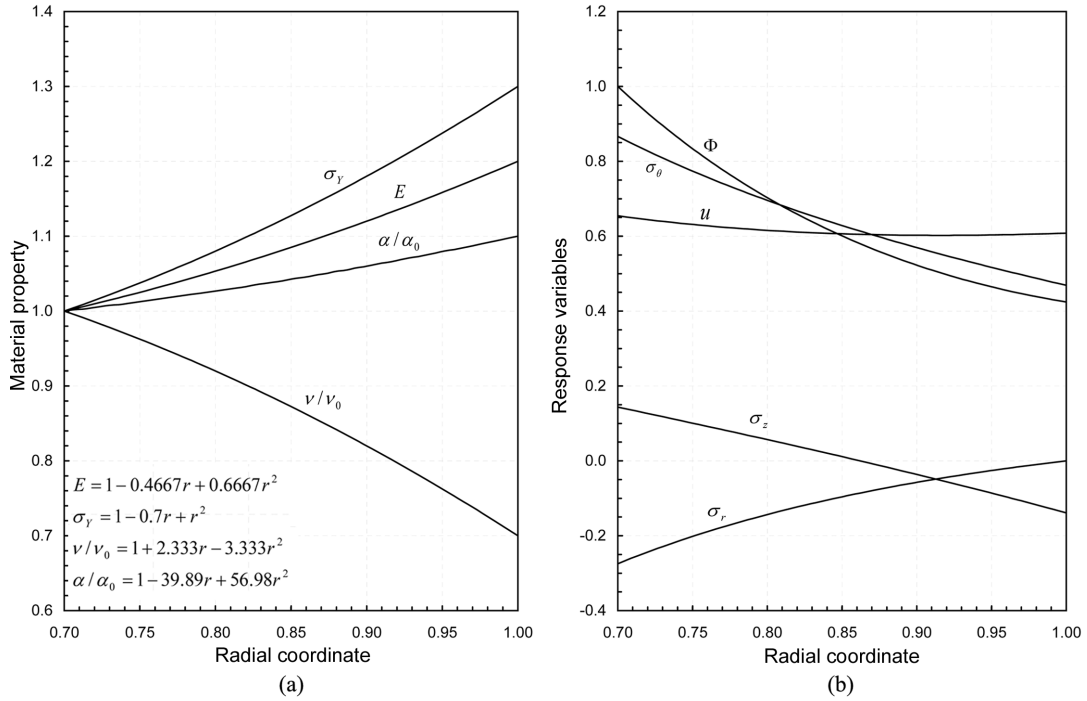


Fig. 3 (a) Variation of E , ν , α and σ_Y in an FGM tube of inner radius $a = 0.7$, (b) the corresponding elastic response for $T_a = 5^\circ\text{C}$, $T_b = 30^\circ\text{C}$ under elastic limit internal pressure

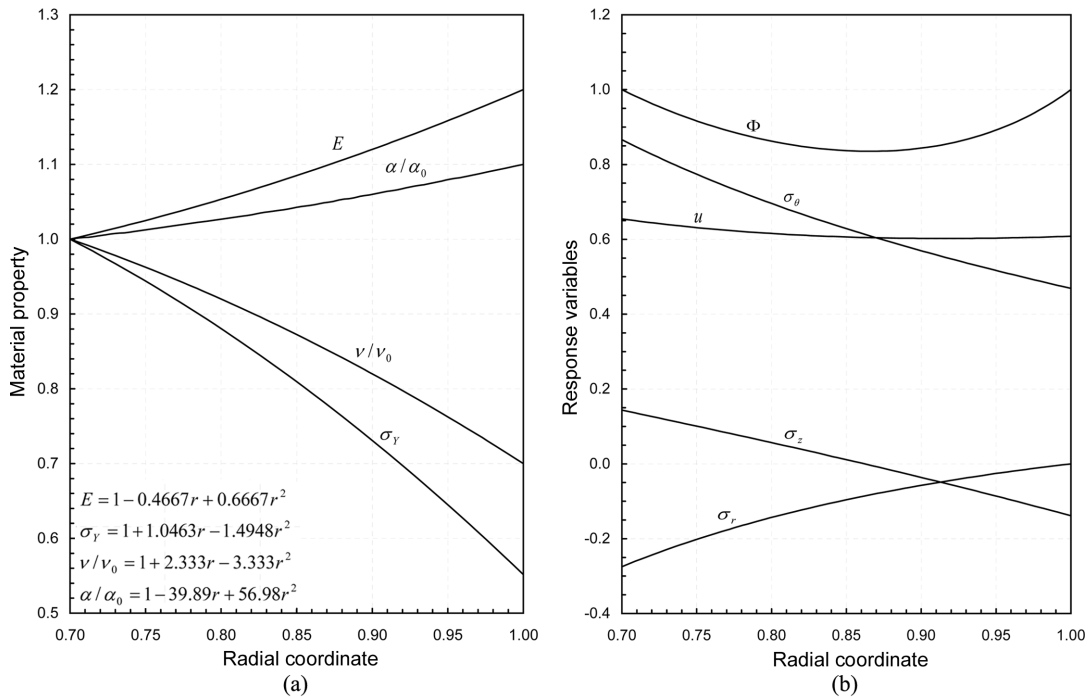


Fig. 4 (a) Variation of E , ν , α and σ_Y in an FGM tube of inner radius $a = 0.7$, (b) the corresponding elastic response for $T_a = 5^\circ\text{C}$, $T_b = 30^\circ\text{C}$ under elastic limit internal pressure

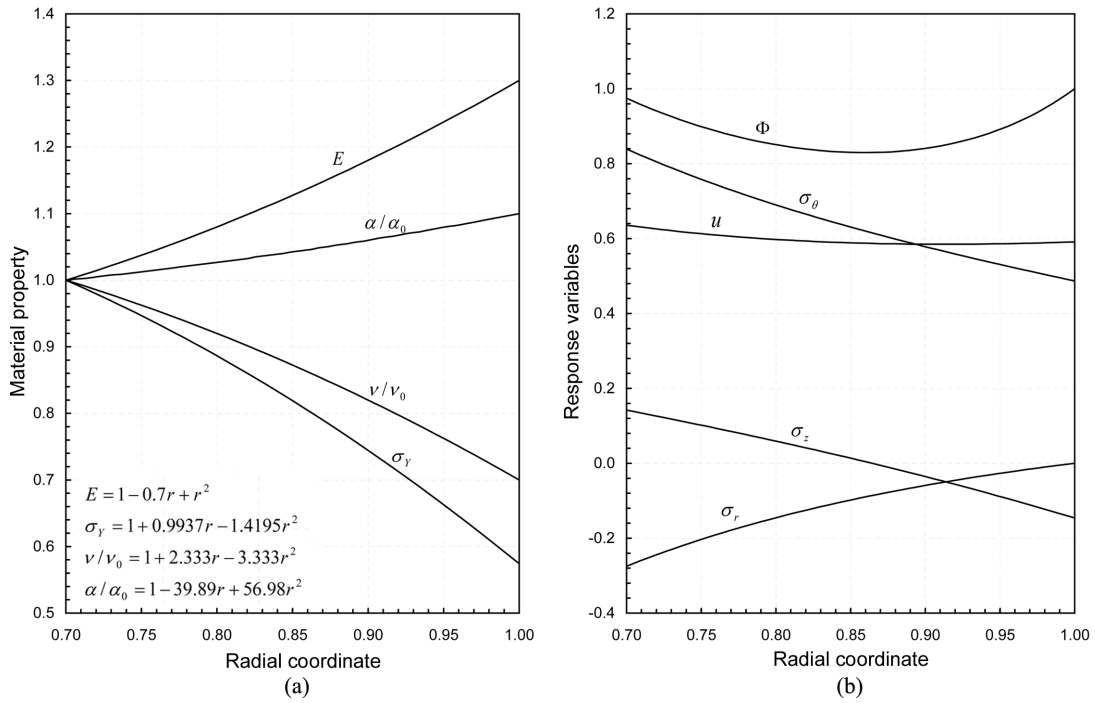


Fig. 5 (a) Variation of E , ν , α and σ_γ in an FGM tube of inner radius $a = 0.7$, (b) the corresponding elastic response for $T_a = 5^\circ\text{C}$, $T_b = 30^\circ\text{C}$ under elastic limit internal pressure

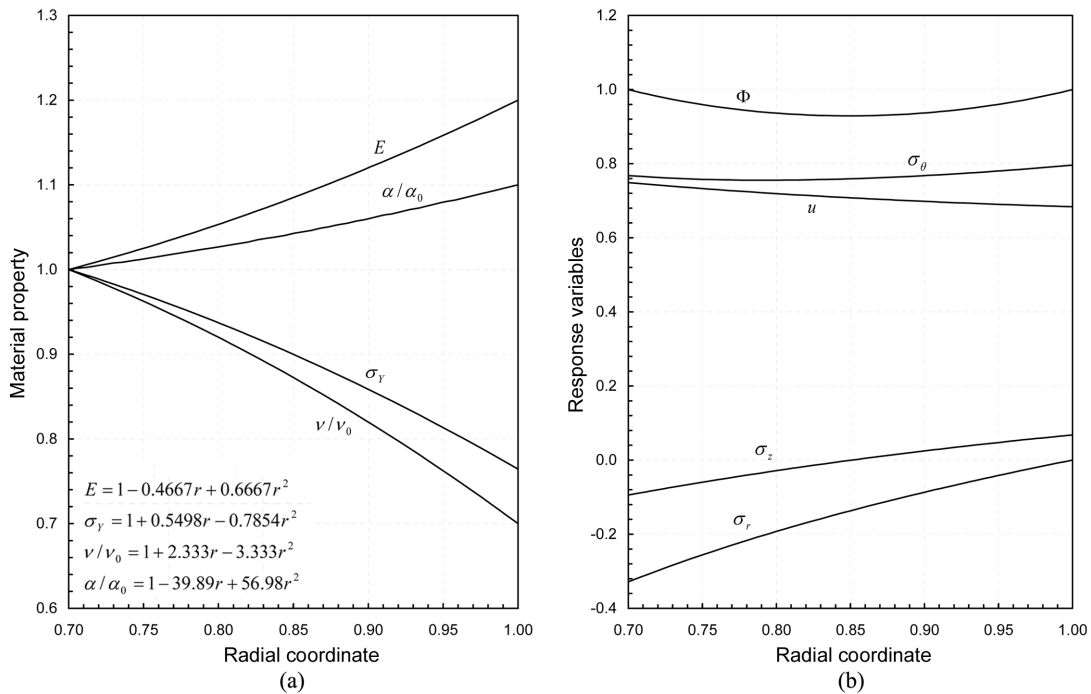


Fig. 6 (a) Variation of E , ν , α and σ_γ in an FGM tube of inner radius $a = 0.7$, (b) the corresponding elastic response for $T_a = 30^\circ\text{C}$, $T_b = 5^\circ\text{C}$ under elastic limit internal pressure

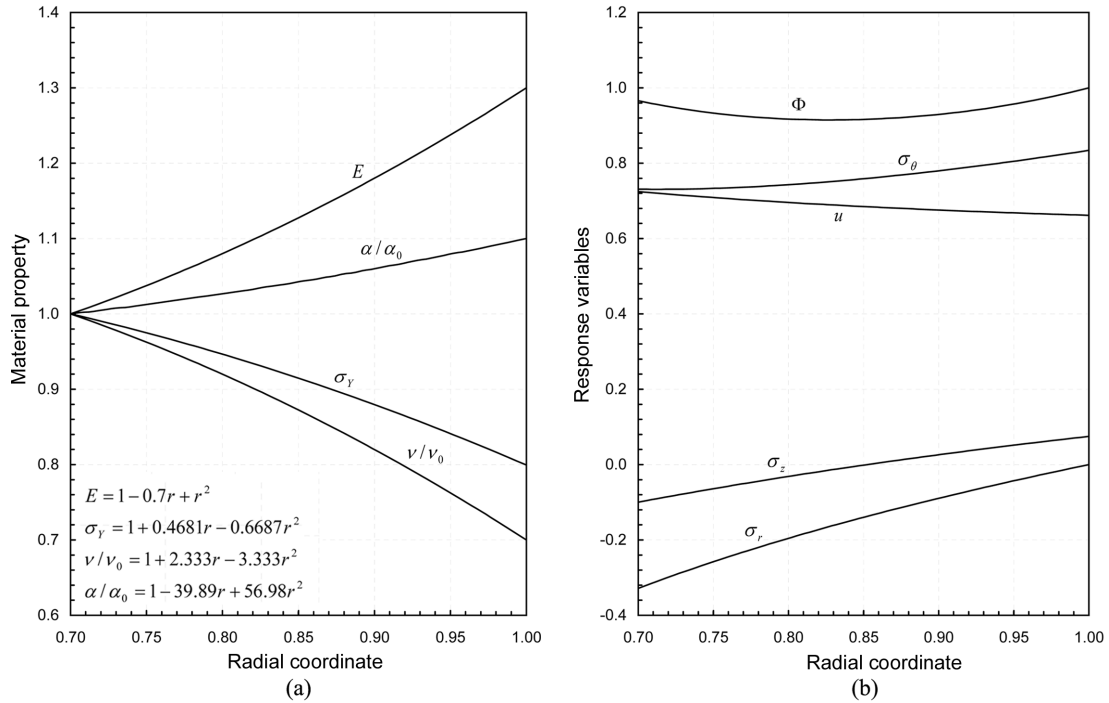


Fig. 7 (a) Variation of E , ν , α and σ_Y in an FGM tube of inner radius $a = 0.7$, (b) the corresponding elastic response for $T_a = 30^\circ\text{C}$, $T_b = 5^\circ\text{C}$ under elastic limit internal pressure

to the distributions of the response variables shown in Fig. 3(b). The variation of the stress variable Φ defined by Eq. (41) makes apparent that under these circumstances the FGM tube yields at the inner surface. If the material composition is changed with that shown in Fig. 4(a), the same tube responds as the one plotted in Fig. 4(b). The tube fails with respect to plastic deformation concurrently at both ends. It is seen by comparing Figs. 3(a) and 4(a) that the only difference between them is in the variation of the yield limit σ_Y . While σ_Y is an increasing function of the radial coordinate r in Fig. 3(a), it decreases with r in Fig. 4(a). The effect of σ_Y on the elastic response of the tube is apparent. As a final example for this tube, we consider the variations of graded properties plotted in Fig. 5(a) and then compute the consequent distributions of the response variables which are plotted in Fig. 5(b). This time yielding commences at the outer surface of the pressurized tube.

Runs are performed for a tube of $a = 0.7$ considering a negative temperature gradient in which $T_a = 30^\circ\text{C}$ and $T_b = 5^\circ\text{C}$. First, the material composition depicted in Fig. 6(a) is taken into account. The corresponding distributions of the response variables at the elastic limit pressure are shown in Fig. 6(b). As seen in this figure, both surfaces are critical and accordingly the tube undergoes plasticization simultaneously at both surfaces as the internal pressure is further increased. The material composition shown in Fig. 7(a), on the other hand, causes the tube to yield at the outer surface as shown in Fig. 7(b).

4.2.2 External pressure

A parametric analysis similar to the one in the preceding section is carried out to find out the

Table 2 Effect of variable E , ν , and α , respectively, on the elastic limit pressure P_E

Property	$\Delta T > 0$	$\Delta T < 0$
$E(a) < E(1)$	$P_E \uparrow$	$P_E \uparrow$
$\nu(a) < \nu(1)$	$P_E \downarrow$	$P_E \downarrow$
$\alpha(a) < \alpha(1)$	$P_E \uparrow$	$P_E \uparrow$

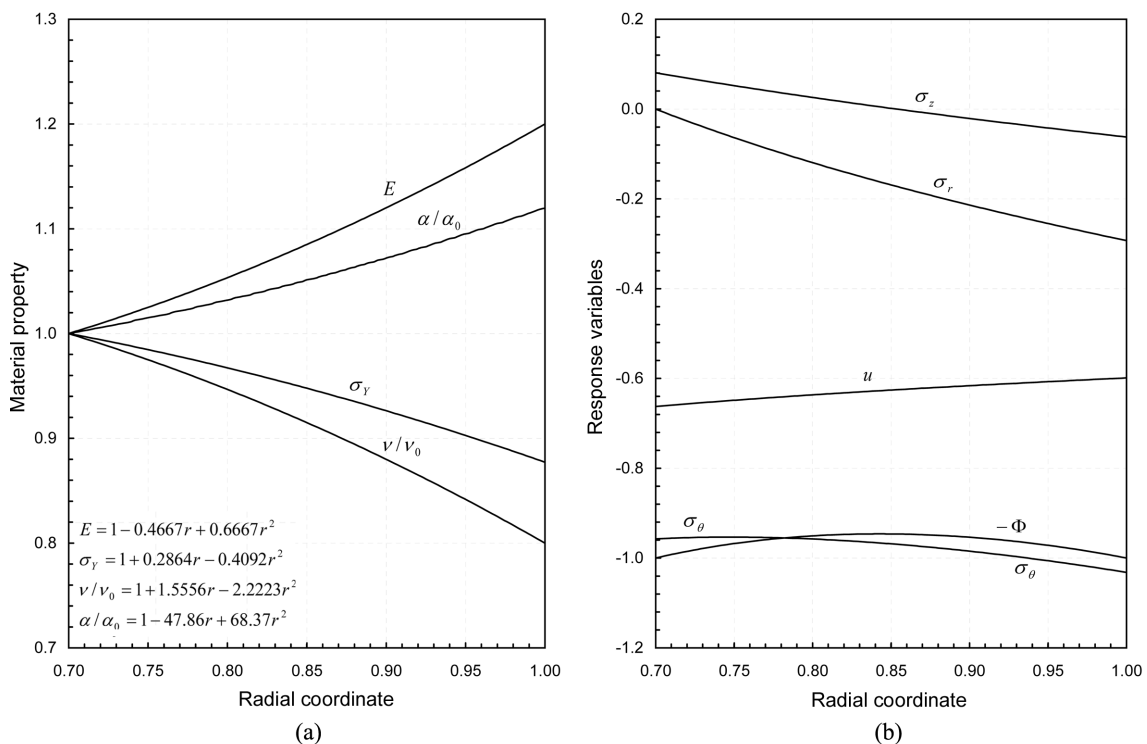


Fig. 8 (a) Variation of E , ν , α and σ_γ in an FGM tube of inner radius $a = 0.7$, (b) the corresponding elastic response for $T_a = 6^\circ\text{C}$, $T_b = 29^\circ\text{C}$ under elastic limit external pressure

effect of each of the variable material properties on the elastic limit pressure P_E . A tube of inner radius $a = 0.7$ and temperature gradients of $\pm 25^\circ\text{C}$, are considered. The results of these calculations can be examined in Table 2. The strength of the tube to resist external pressure elastically increases if E or α is an increasing but the Poisson's ratio ν is a decreasing function of r irrespective of the sign of ΔT .

Like in the internal pressure case, different FGM compositions leading to different modes of incipient yielding are possible. For example, the composition shown in Fig. 8(a) for the tube of $a = 0.7$, $T_a = 5^\circ\text{C}$ and $T_b = 30^\circ\text{C}$ gives rise to the elastic response shown in Fig. 8(b). Plasticization initiates at both of the surfaces at the same time, whilst a homogeneous one always yields at the inner surface as shown in Fig. 2. If the tube material is changed with that shown in Fig. 9(a), plasticization initiates at the outer surface of the tube as depicted in Fig. 9(b).

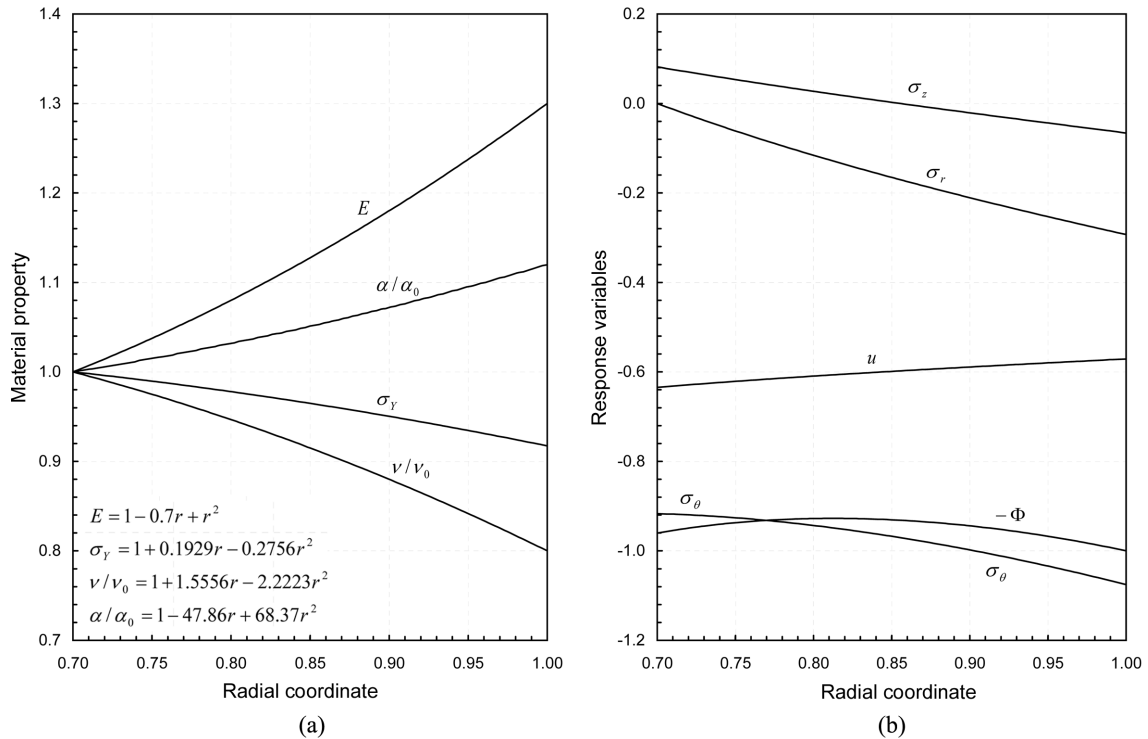


Fig. 9 (a) Variation of E , ν , α and σ_Y in an FGM tube of inner radius $a = 0.7$, (b) the corresponding elastic response for $T_a = 6^\circ\text{C}$, $T_b = 29^\circ\text{C}$ under elastic limit external pressure

5. Conclusions

Functionally graded materials (FGM) have been widely used for the last two decades particularly in high temperature and industrial applications, in microelectronics, and in power transmission equipment. Among various advantages of using FGM, increasing strength, toughness, endurance limit, and resistance to corrosion, and retardation of the development of surface cracks can be cited. In spite of these advantages, the stresses in FGM pressurized tubes have not been well studied theoretically.

In this study, an efficient, yet simple, computational model is developed to perform stress analysis concerning the elastic response of a plane strain thick walled FGM tube subjected to both pressure and a small temperature gradient. The modulus of elasticity, the Poisson's ratio, the yield strength, and the coefficient of thermal expansion, are assumed to vary nonlinearly in the tube. Moreover, the deformation in the axial direction is allowed. Under these conditions, the preheated FGM tubes subjected to either internal or external pressure are studied in detail. It is observed that, although small temperature gradients (of the order of $\pm 25^\circ\text{C}$) and reasonable variations of material properties are considered, the states of stress are affected significantly by both the material nonhomogeneity and the existence of a small temperature gradient. Material compositions leading to different modes of incipient yielding are shown to be possible. A preheated FGM pressure tube may yield at the outer surface or simultaneously at both surfaces, whilst a homogeneous one always yields at the

inner surface. All graded properties affect the elastic response of the tube to some extent, though, the effects of the modulus of elasticity and the yield strength are observed to be highly pronounced. In this sense, for example, the elastic performance of the tube is substantially increased if the modulus of elasticity is chosen to be an increasing function of the radial coordinate. However, since the material compositions are chosen rather arbitrarily in this work, further study may be carried out to optimize the performance by treating the material parameters as design variables in the optimum design problem.

Acknowledgements

The author takes this opportunity to thank Ms. Yeşim Çöteli in the Department of Modern Languages at METU for editing the manuscript with care and patience to improve its language. Mr. Tunç Apatay, a Ph.D., student in the ME Department at Gazi University, has been helpful during the course of this work. His help is greatly appreciated.

References

- Akis, T. and Eraslan, A.N. (2005), "Yielding of long concentric tubes under radial pressure based on von Mises criterion (In Turkish)", *J. Faculty Eng. Arch. of Gazi Univ.*, **20**, 365-372.
- Boley, B.A. and Weiner, J.H. (1960), *Theory of Thermal Stresses*, Wiley, New York, .
- Boresi, A.P., Schmidt, R.J. and Sidebottom, O.M. (1993), *Advanced Mechanics of Materials*, 5th. ed. Wiley.
- Brown, P.N. and Hindmarsh, A.C. (1989), "Reduced storage matrix methods in stiff ODE systems", *Appl. Math. Comput.*, **31**, 40-91.
- Eraslan, A.N. and Akis, T. (2004), "Deformation analysis of elasto-plastic two layer tubes subject to pressure: An analytical approach", *Turkish J. Eng. Envir. Sci.*, **28**, 261-268.
- Eraslan, A.N. and Akis, T. (2005a), "Elastoplastic response of a long functionally graded tube subjected to internal pressure", *Turkish J. Eng. Envir. Sci.*, **29**, 361-368.
- Eraslan, A.N. and Akis, T. (2005b), "Yielding of two layer shrink-fitted composite tubes subject to radial pressure", *Forschung im Ingenieurwesen/Eng. Res.*, **69**, 187-196.
- Eraslan, A.N. and Akis, T. (2006), "Plane strain analytical solutions for a functionally graded elastic-plastic pressurized tube", *Int. J. Pressure Vessels Piping*, **83**, 635-644.
- Horgan, C.O. and Chan, A.M. (1999), "The pressurized hollow cylinder or disk problem for functionally graded isotropic linearly elastic materials", *J. Elast.*, **55**, 43-59.
- Jabbari, M., Sohrabpour, S. and Eslami, M.R. (2002), "Mechanical and thermal stresses in a functionally graded hollow cylinder due to radially symmetric loads", *Int. J. Pressure Vessels Piping*, **79**, 493-497.
- Ma, L., Feng, X.Q., Gau, K.W. and Yu, S.W. (2003), "Elastic and plastic analyses of functionally graded elements", *Functionally Graded Materials VII Materials Science Forum*, **423-4**, 731-736.
- Mendelson, A. (1986), *Plasticity: Theory and Application*. MacMillan.
- Nadai, A. (1931), *Plasticity*, Mc-Graw-Hill.
- Parker, A.P. (2001), "Autofrettage of open-end tubes - Pressures, stresses, strains, and code comparisons", *J. Pressure Vessel Technol. - Transactions of the ASME*, **123**, 271-281.
- Perry, J. and Aboudi, J. (2003), "Elasto-plastic stresses in thick walled cylinders", *J. Pressure Vessel Technol. - Transactions ASME*, **125**, 248-252.
- Timoshenko, S.P. (1956), *Strength of Materials: Part II Advanced Theory and Problems*, 3rd. ed. D. van Nostrand Company.

- Timoshenko, S.P. and Goodier, J.N. (1970), *Theory of Elasticity*, 3rd. ed. McGraw-Hill.
- Tutuncu, N. and Ozturk, M. (2001), "Exact solutions for stresses in functionally graded pressure vessels", *Composites: Part B*, **32**, 683-686.
- Ugural, A.C. and Fenster, S.K. (1987), *Advanced Strength and Applied Elasticity*, 2nd. SI ed. Prentice Hall.